SF2A 2021
A. Siebert, K. Baillié, E. Lagadec, N. Lagarde, J. Malzac, J.-B. Marquette, M. N'Diaye, J. Richard, O. Venot (eds)

REVEALING NEW WORLDS FROM DARKNESS: GLINT

M.-A. Martinod[1]

Abstract. Characterisation of exoplanets is key to understanding their formation, composition and potential for life. However, detecting their glint drown in the overwhelming star glare is challenging. Nulling interferometry, combined with extreme adaptive optics, is among the most promising techniques to address it and advance this goal. We present an integrated-optic nuller whose design is directly scalable to future science-ready interferometric nullers: the Guided-Light Interferometric Nulling Technology, deployed at the Subaru Telescope. It combines four beams and delivers spatial and spectral information. We demonstrate the capability of the instrument on-sky. These successes pave the way for future design enhancements: scaling to more baselines, improved photonic component and handling low-order atmospheric aberration within the instrument, all of which will contribute to enhanced sensitivity and precision.

Keywords: Nulling, interferometry, high contrast imaging, high angular resolution, GLINT, exoplanets, integrated-optics, photonics, adaptive-optics

1 Introduction

Despite more than 4800 detected exoplanets so far, few are detected within the habitable zone or the snow line (Fig. 1). The latter region is critical for studying the formation process of planetary systems where young Jupiter-like exoplanets are mainly located (Fernandes et al. 2019). However, most exoplanets have been discovered by indirect methods (such as transits or radial velocities), which tends to detect giant planets close to their host star, or by direct imaging (e.g. coronagraphy), which tends to detect planets far from their star. Accessing the intermediate scale where the snow line necessitates high angular resolution and high contrast capabilities.

The technique of nulling interferometry addresses both issues: it suppresses the overwhelming glare of the host star while preserving the light of the planet. This technique makes the on-axis starlight self-destructively interfere (Bracewell 1978) by setting a π radians phase shift. The light coming from an off-axis source carries another phase shift imposed by the non-axial angle of incidence. Thus, it does not destructively interfere inside the nulling interferometer and can be detected.

Unlike coronagraphs, the effective Inner Working Angle (IWA) of a nuller depends on the baseline B separating the apertures so that $IWA = \frac{\lambda}{2B}$ (Lay 2005). Furthermore, the spatial structure can still be resolved below the IWA at the expense of lower achievable contrast.

The primary observable is called the *null depth*, defined as the ratio of the intensity of destructive over constructive interference. It quantifies the degree of suppression of the light due to the spatial brightness distribution of the source.

The *Guided-Light Interferometric Nulling Technology* (GLINT) is the first nuller based on integrated-optics technology to perform light processing. It is deployed at the Subaru Coronagraphic Extreme Adaptive Optics system (SCExAO) (Guyon et al. 2011; Jovanovic et al. 2015), at the Subaru Telescope, which provides wavefront correction.

We present the instrument in Section 2 and its on-sky commissioning in Section 3 and the further upgrades and applications allowed by the use of integrated optics in Section 4.

[1] University of Sydney, 2006, Sydney, NSW, Australia

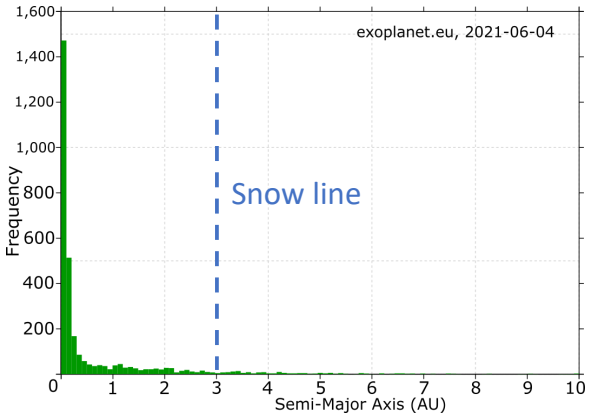

Fig. 1. Histogram of discovered of exoplanets with respect to the semi-major axis in AU. The vertical blue dashed-line is the snow-line for a Sun-like star.

2 Presentation of GLINT

GLINT and its commissioning in lab and on-sky have been extensively described in Martinod et al. (2021a). In a nutshell, GLINT is optimised for science by benefiting from the wavefront correction provided by the extreme adaptive optics system (AO) of SCExAO and being the first instrument able to cancel several baselines simultaneously. GLINT operates in the H band and disperses the light from 1400 to 1650 nm with a spectral resolution of 160 at 1.55 μm. GLINT combines up to 4 apertures, providing 6 non redundant baselines, spanning from 2.15 to 6.45 metres. The light processing is performed inside an integrated-optics component which has two functions. The first one is to coherently remap the 2D configuration of the aperture mask into a linear array. The second function is to combine the beams pair-wise with directional couplers and provides photometric outputs. The former delivers information about the injection for each aperture. The latter delivers two outputs per baseline in opposition of phase: one 'null' output carrying the destructive interference (in which the planet-light will be) and an 'antinull' output carrying the constructive interference (which mainly contains the starlight). The integrated-optic chip is designed with the Ultrafast Laser Inscription method (ULI) (Nolte et al. 2003; Gattass & Mazur 2008; Arriola et al. 2013; Gross & Withford 2015) which allows three-dimensional circuitry. The 16 outputs are spectrally dispersed on a CRED2 InGaAs camera, operating at 0.7 ms to 'freeze' the atmospheric turbulence.

The data processing relies on the *Numerical Self-Calibration* method described by Hanot et al. (2011) adapted for the case of multiple baselines and spectral dispersion. To sum up, this method models the statistical fluctuations of the measured null depth to determine the null depth of the source (called 'source null depth' hereafter) without a calibrator. The main advantage of such a method is a longer observing time of the object of interest. The disadvantages so far are the need for an extensive dataset ($>10^5$ frames) and a high signal-to-noise ratio per frame.

3 On-Sky commissioning

GLINT was deployed on-sky to determine the apparent angular diameters of α Bootis and δ Virgo.

α Bootis is a red giant branch star, with magnitude in H band of -2.81 mag and with published angular diameter measurements between 19.1 and 20.4 mas (Richichi et al. 2005) in K band. It is around 40% of the λ/D diffraction limit of the telescope in our band. The average seeing during the night of the 20th of June 2020 ranged between 0.3 and 0.5 arcseconds at 1600 nm, but with some significant wavefront error resulting from low-wind-effect and telescope vibrations. Data was acquired for 15 min at a frame rate of 1400 Hz for four baselines spanning from 2.15 to 5.68 metres.

δ Vir is also a red giant branch star, with a magnitude in H band of -1.05 mag and a measured angular diameter of 10.6 ± 0.736 mas in H band (Bourges et al. 2017), i.e. around 20% of the diffraction limit. The conditions of observation for the night of the 5th of July 2020 and the configuration of the acquisition were the same as for α Bootis.

For each star, the source null depth was determined with respect to the four baselines with the NSC method. The angular diameters of both stars were deduced from the fit of these four null depths by a uniform disk model that gave the expected null leakage given the stellar size.

The source null depth points of α Boo are an excellent match to the expected curve and yield parameters within the range of expected literature values (Fig. 2, left). The angular diameter found is 19.7 ± 0.1 mas with a reduced χ^2 of 52.0. The uncertainty has been rescaled by the square root of the reduced χ^2. The χ^2 is high because the error bars are derived only from statistical diversity in the data and do not account for systematics (for example, blurring due to seeing variations faster than the frame rate).

Similarly, the found diameter of δ Vir is 10.9 ± 0.1 mas with a reduced χ^2 of 11.2 where the uncertainty has been rescaled as before. The source null data points yield an excellent fit to the model (Fig. 2, right), which in turn is in agreement with literature expectations for this star (expected UD diameter of 10.6 mas). As for α Boo, the high χ^2 betrays the presence of systematic errors not taken into account in the measurement of the null depth.

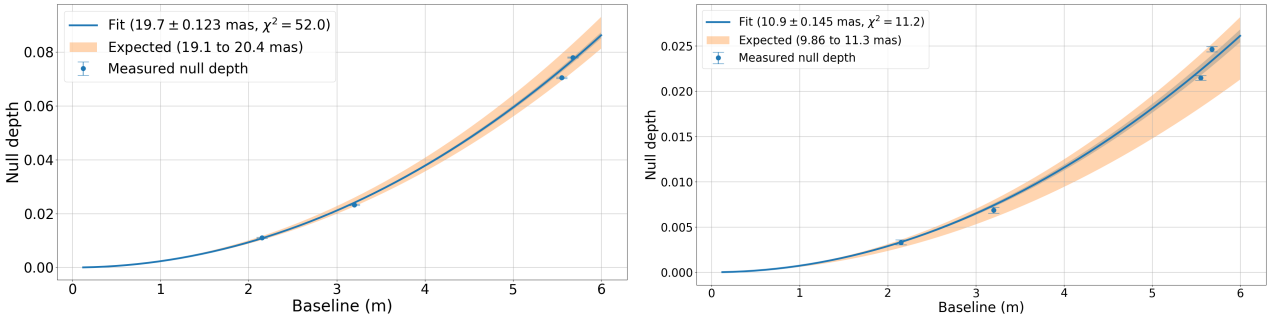

Fig. 2. Left: Variation of the source null depth of α Boo (blue dots) as a function of baseline together with the best-fit model (blue solid curve). The orange area highlights the expected range of null depth at 1550 nm for an expected UD diameter between 19.1 and 20.4 mas. Right: Source null depth of δ Vir (blue dots) with baseline together with the best-fit model (blue solid curve). The orange gives the expected range of null depth for a UD diameter between 9.86 and 11.3 mas. The error bars on both plots represent the standard deviation of the fitted value of the source null depth given by the covariance matrix of the fit of the histogram, rescaled by the reduced χ^2 of that fit.

4 Further upgrades and applications

The directional coupler is a chromatic device that limits the null depth to achieve the desired contrast of 10^{-5} to detect self-luminous exoplanets. In addition, extreme adaptive optics suffer from low-order aberrations (Vievard et al. 2020) which are sharp phase discontinuities across the telescope's spiders believed due to thermal effects. The pyramid wavefront sensor of SCExAO is blind to this effect, but GLINT is (Fig. 3). It shows the potential for a photonic instrument nuller also to be used as a wavefront sensor. These two elements are the main limiting factors of the performance of GLINT and will be addressed in a future upgrade with the replacement of the directional couplers by tricouplers.

The concept of the tricoupler could solve both issues as it provides an achromatic null depth and fringe-tracking capabilities while performing nulling. This all-in-one device is interesting as it is not affected by non-common-path errors and can be used as a wavefront sensor to enhance the wavefront correction of an AO system. Its application has been explored by Martinod et al. (2021b).

In a nutshell, a tricoupler where three parallel guides are at the points of an equilateral triangle provide interesting symmetry properties for a nuller. If the incident beams can be injected in anti-phase, then the intrinsic symmetry of the structure means that none of the light is able to couple into the central guide regardless of the wavelength. For nulling, this centre waveguide is exploited as the null channel. The outer waveguides will allow recovering the incoming beams' differential phase, thus feeding a fringe tracker or the AO system to stabilize the null depth. This ability will allow an AO system to correct low-order aberrations.

The simulations of a GLINT instrument with tricoupler performing fringe tracking instead of directional coupler presented by Martinod et al. (2021b) show a gain of the null depth by a factor of 45. This device, added to the NSC for data processing, would allow reaching the required contrast of 10^{-5} to image exoplanets.

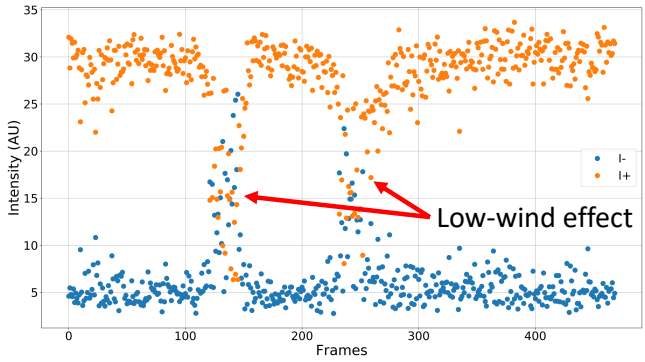

Fig. 3. Fluxes measured at the null (blue dots) and antinull (orange dots) outputs of the baseline of 5.55 metres. The events when the outputs swap are due to low-wind effect.

5 Conclusion

GLINT is the first nuller based on integrated-optic technology combining more than two apertures and providing spectral information. It successfully measured the diameter of stars which are respectively smaller than the half and the quarter of the diffraction limit of the telescope. It demonstrates the potential of this technology, associated with adaptive optics, to design instruments able to image and characterize exoplanets within the snow line. The use of integrated-optics device makes the concept easily scalable to bigger telescopes or long-baseline interferometry. The current limitations of GLINT have been identified and are being addressed with the investigation and the development of the photonic tricoupler which provides an achromatic signal and fringe-tracking capability.

M.A. Martinod acknowledges funding through the Australian Research Council Discovery Program DP180103413.

References

Arriola, A., Gross, S., Jovanovic, N., et al. 2013, Optics Express, 21, 2978

Bourges, L., Mella, G., Lafrasse, S., et al. 2017, VizieR Online Data Catalog, II/346

Bracewell, R. N. 1978, Nature, 274, 780

Fernandes, R. B., Mulders, G. D., Pascucci, I., Mordasini, C., & Emsenhuber, A. 2019, ApJ, 874, 81

Gattass, R. R. & Mazur, E. 2008, Nature Photonics, 2, 219

Gross, S. & Withford, M. J. 2015, Nanophotonics, 4, 20

Guyon, O., Martinache, F., Clergeon, C., et al. 2011, Society of Photo-Optical Instrumentation Engineers (SPIE) Conference Series, Vol. 8149, Wavefront control with the Subaru Coronagraphic Extreme Adaptive Optics (SCExAO) system, 814908

Hanot, C., Mennesson, B., Martin, S., et al. 2011, ApJ, 729, 110

Jovanovic, N., Martinache, F., Guyon, O., et al. 2015, PASP, 127, 890

Lay, O. P. 2005, Appl. Opt., 44, 5859

Martinod, M.-A., Norris, B., Tuthill, P., et al. 2021a, Nature Communications, 12, 2465

Martinod, M.-A., Tuthill, P., Gross, S., et al. 2021b, Appl. Opt., 60, D100

Nolte, S., Will, M., Burghoff, J., & Tuennermann, A. 2003, Applied Physics A: Materials Science & Processing, 77, 109

Richichi, A., Percheron, I., & Khristoforova, M. 2005, A&A, 431, 773

Vievard, S., Bos, S. P., Cassaing, F., et al. 2020, in Society of Photo-Optical Instrumentation Engineers (SPIE) Conference Series, Vol. 11448, Society of Photo-Optical Instrumentation Engineers (SPIE) Conference Series, 114486D